J Mater Sci (2007) 42:7812–7818
DOI 10.1007/s10853-007-1591-0

Microstructure and infiltration kinetics of Si_3N_4/Al–Mg composites fabricated by pressureless infiltration

Shou-ren Wang · Ying-zi Wang · Yong Wang · Hao-ran Geng · Qing Chi

Received: 21 October 2006 / Accepted: 2 February 2007 / Published online: 24 May 2007

Abstract Si_3N_4/ Al–Mg composites reinforced by ceramic interpenetrating network structure had been fabricated via pressureless infiltration technology. The matrix and the reinforcement phase, form an interconnected interpenetrating network structure. The Al–Mg/Si_3N_4 system exhibits an excellent wettability under moderate conditions. The increasing of Mg content (2–10 wt%) resulted in an increased amount of infiltration, once Mg content beyond 10 wt% has an adverse effect. Light chemical reaction occurs in the interface of Al–Mg/Si_3N_4 system and the reaction productions reduce the surface tension of melt and impulse the advance of infiltration. Infiltration temperature and infiltration time were the key parameters, which turn into the infiltration impetus. The appropriate infiltration temperature is 1050 °C and the corresponding infiltration time is 15 min, prolonging the infiltration time continuously has no significance.

Introduction

Metal matrix composites (MMCs) have some kinds of reinforcements such as particle, whisker and fibre [1–3] as well as three-dimensional network structure [4]. In recent years, three dimensional (3-D) network structure reinforced aluminum magnesium matrix composites (3-DNRMMCs) have been receiving much attention, since they possess rather high specific strength and stiffness, wear-resistance, excellent thermal and electrical conductivities and can be an attractive candidate for structural and functional materials [5]. There are several methods to fabricate 3-DNRMMCs including stir casting (SC) [6, 7], mechanical alloying (MA) [8], powder metallurgy (PM) [9], squeeze cast (SQC) [10], molten metal infiltration (MMI) [11] and self-propagating high-temperature synthesis (SHS) [12–13]. Among all the techniques, infiltration methods is the only technique suitable for fabricating high volume fraction (>50%) MMCs and infiltration technology is the most attractive processing route to fabricate 3-DNRMMCs, which can be classified into three categories based on the source of driving force: pressure assisted, vacuum driven and pressureless or capillarity driven infiltration [14]. Moreover, the infiltration technology for 3-DNRMMCs have more advantage, for example, the metal phase fraction, size, shape, and distribution can be controlled through consolidation and densification processing of porous skeleton. Infiltration with metal can yield dense composites without the large shrinkage associated with liquid phase sintering [15].

Among all infiltration technology, pressureless infiltration is the most attractive because of its spontaneousness, low-cost and simpleness. However, spontaneous infiltration requires an excellent wetting of network structure by molten metals. Improving the wettability to boost spontaneous infiltration is the key route for 3-DNRMMCs fabrication. Now less work has been carried out on the spontaneous infiltration of 3-DNRMMCs, so in the present paper, the infiltration kinetics of 3-DNRMMCs was

S.-r. Wang (✉) · Q. Chi
School of Mechanical Engineering, Jinan University, Jinan 250022, P. R. China
e-mail: sherman0158@tom.com

Y.-z. Wang · H.-r. Geng
School of Material Science, Jinan University, Jinan 250022, P. R. China

Y. Wang
School of Science, Jinan University, Jinan 250022, P. R. China

investigated. The purpose of this study is to describe the mechanisms of spontaneous infiltration of Si_3N_4/Al–Mg composites.

Experimental procedure

Fabrication of porous ceramic skeleton

High-purity β–Si_3N_4 powder (characteristics of Si_3N_4 powder are shown in Table 1) was used as starting material for fabrication of porous ceramic skeleton. The sintering additives including 2 wt%Al_2O_3, 5 wt%ZrO_2 and 5 wt%Al were mixed with the starting material and ball-milled for 4 h using Al_2O_3 balls. A reticulated polymeric sponge as preceramic materials with interconnected pores was chosen to prepare the porous preform by the replica process. The cleared sponge was cut into standard form of $\varphi 30 \times 100$ mm and immersed into the homogeneous slurry for about 10 min. the samples were placed into the drying stove and dried for 20 h at 160 °C to remove most of the moisture, and then, sintering process was carried through at 1400 °C for 2 h in oxidizing atmosphere.

Fabrication of Si_3N_4/Al–Mg composites

Commercial purity Al ingot (99.7% in wt.) and Mg ingot (99.95% in wt.) were used to prepare the Al–Mg alloys by melting in clay–graphite crucible. Element Mg was wrapped with Al foil in order to prevent evaporation losses and Mg content was 2, 5, 8, 10, and 14 wt%, respectively. The porous Si_3N_4 ceramic skeletons were heated up in an furnace under Ar atmosphere together with the infiltration die. After achieving the appointed temperature, the liquid metal was infiltrated into the infiltration die.

Characterization

The morphologies and fracture surface characteristic of the reticulated porous ceramics (RPCs) were characterized by a scanning electron microscopy (SEM, Hitachi, No.S-2500). The density and porosity were measured using Archimedes'method (ASTM C373-00). The pore size was determined by the bubble method. In this method the pore size is defined by the pressure required for the first air bubble to be pressed out by the porous sample. Chemical element distributions were examined by the energy spectrum analyses (ESA, OXFOED INCA). The surface morphology and fractographs of 3-DNRMMCs was performed on a scanning electron microscope (SEM. Hitachi, S-2500). The wetting angles in Al melt with different Mg content and Si_3N_4 substrate were measured through sessile drop technique. Weight gains were examined by thermo-analytical balance.

Table 1 Characteristics of Si_3N_4 powder wt%

Si	N	O	CaO	Fe_2O_3	MnO	TiO_2	NiO
59.25	37.27	1.15	0.17	0.58	0.13	0.018	0.013

Results and discussion

Microstructure of skeleton and composites

Si_3N_4 offered the potential for development as a high strength, high temperature refractory material, so it is the appropriate and preferred materials as the reinforcement of metal matrix composites. However, it was soon recognized that pure Si_3N_4 could not be fabricated into fully dense components because of its strong covalent bonding. Alternative methods have therefore been explored and one of the most successful fabrication techniques is liquid phase sintering using a metal silicon oxynitride based liquid. For this purpose it is necessary to add small amounts of metal oxides, which at sintering temperature react with the natural surface SiO_2 on the Si_3N_4 powder, particles and with the Si_3N_4 itself, to form a liquid. The liquid phase assists particle rearrangement and acts as a high diffusivity pathway for the subsequent solution–diffusion–precipitation process. Generally, the constituents of this liquid phase cannot be completely incorporated into the Si_3N_4 lattice, and they remain either as a glass, or as a crystalline metal silicon oxynitride phase in the intergranular region of the Si_3N_4 ceramic [16]. This is the purpose to apply additives as Al_2O_3, ZrO_2, Al powder in the test processes. The intrinsic properties of a material, especially at high temperature, are determined by the content and type of sintering additive; different sintering aids yield different phase compositions and microstructures. Al as low temperature sintering additives was melted and oxidized into Al_2O_3 in the course of sintering and jammed the hollow struts. Al_2O_3 as high temperature sintering additives would improve the density of struts. Figure 2 shows the representative morphology of Si_3N_4 RPCs. Owing to the disappearance of polymer precursor, a big triangular void in the centre of struts (arrow marked in Fig. 1) occurred and some micro-void distributed in all the cross-section of struts (Fig. 2a). Owing to the existence of additives, mostly void in the centre of struts lose the sharp edged features and exhibited a round appearance (arrow marked in Fig. 2a). The distributions of start materials and sintering additives are not homogeneous which was shown in the higher magnifications of struts in Fig. 2a. Chemical element distributions examined by the energy spectrum analyses

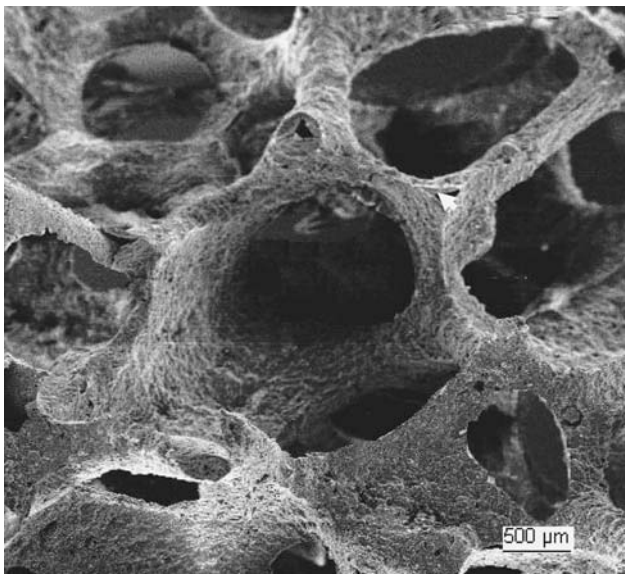

Fig. 1 The morphology of Si_3N_4 reticulated ceramics perform

(1,2,3 point) were shown in Fig. 2b–d. This phenomenon validated the fluxion of glass phase around the Si_3N_4 particle. The average pore diameter(d), the density of porous structure (ρ_*), the density of the fully dense material (ρ_s), the relative density of porous ceramic (ρ_r), the open porosity (ϕ_1) and the close porosity (ϕ_2) are shown in Table 2.

A typical microstructure of 3-DNRMMCs is shown in Fig. 3. The metal phase fills the pores of RPCs homogeneously. The region marked 1 is Si_3N_4 ceramic skeleton, the region marked 2 is Al–Mg metal matrix phase and the region marked 3 is the interface of both phase. It is interest for light weight metal as interpenetrating phase to infiltrate into RPCs. Si_3N_4 fillers can be added to modify the microstructure and to adjust the mechanical and thermal properties of 3-DNRMMCs. RPCs offer a higher interconnectivity of the cells and a higher isotropy of the cell arrangement compared to the conventional porous ceramic fabrication technology. It can be shown form Fig. 3 that both phases, the matrix and the reinforcement phase, form an interconnected interpenetrating network structure.

Infiltration kinetics

Wetting angle and infiltration force

The wettability of Si_3N_4 by Al–Mg melt is indicated by the contact angle between the two phases. If the melt drop spread completely over the Si_3N_4 face, contact angle $\theta = 0°$ and ideal wetting occurs. In a non-wetting system contact angle is 180°. $\theta = 90°$ was taken as the critical wetting angle for pressureless infiltration, so the wetting of ceramic by melt is critical for the processing of 3-DNRMMCs. It is indicated according the Young–Duper

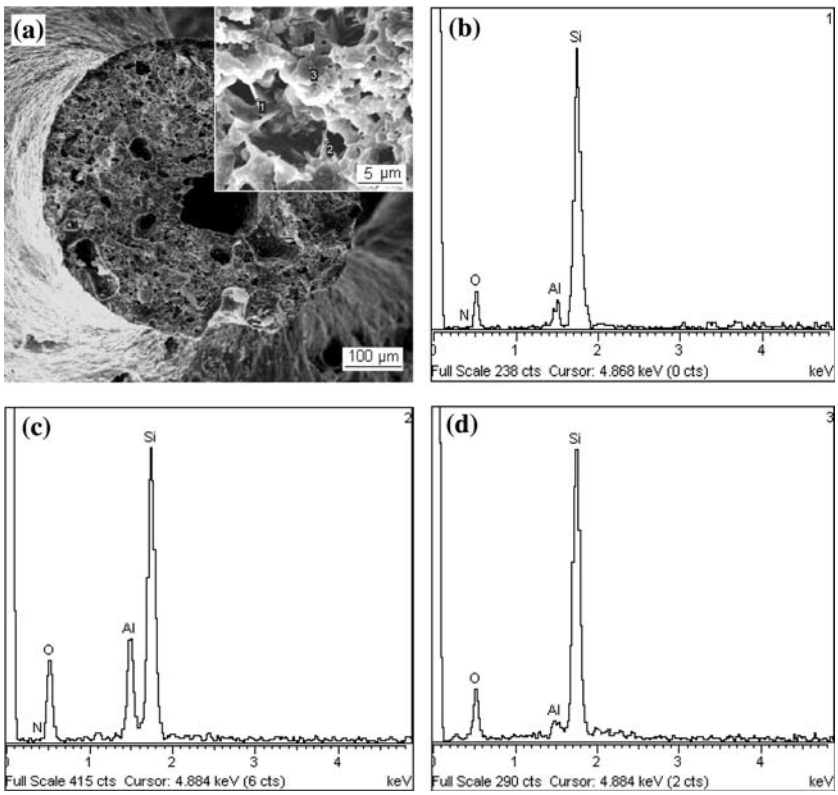

Fig. 2 The morphology of Si_3N_4 reticulated ceramics perform

Table 2 The density and porosity of porous ceramic skeleton

d (mm)	ρ^*(g/cm^3)	ρ_s (g/cm^3)	ρ_r	ϕ_1 (%)	ϕ_2 (%)
1–3	0.51	3.17	0.16	2.6	84

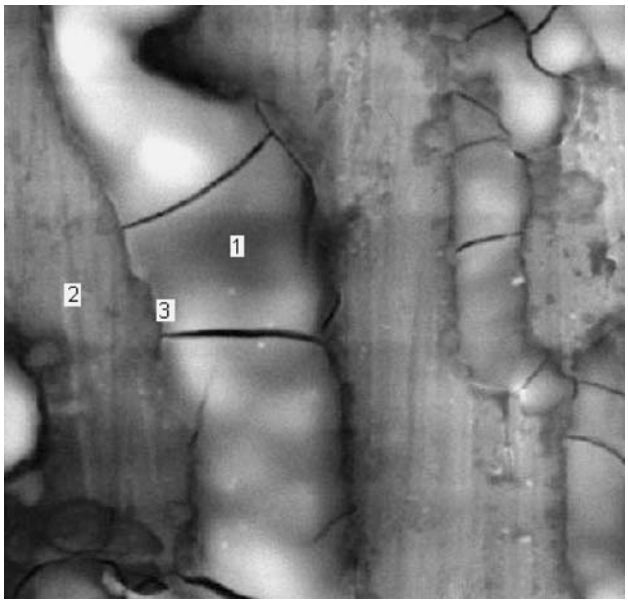

Fig. 3 The microstructure of 3-DNRMMCs

equation that melt begin to wet the template Si_3N_4 face once the wetting angle θ<90°. The wetting angles decrease gradually with the increases of temperature. From Fig. 4, when the temperature exceeds about 800 °C, the wetting angles are smaller than 90° (2–10% Mg). When the temperature is about 900 °C, the angle is 55° (5% Mg). When the temperature is about 1000 °C, the angle is 30° (5% Mg) and when the temperature is about 1050 °C, the angle is 25° (5% Mg). With the temperature continuously increases (>1050 °C), the wetting angle no longer decreases, moreover, the wetting angle sometimes increases from some test data analyses, there may be the reason that the reaction productions increase the viscosity of melt, this needs validated in further tests in the future.

The Laplace–Young equation predict the infiltration force as follow,

$$\Delta P = \frac{2\sigma_{lg}\cos\theta}{r} \quad (1)$$

where σ_{lg} is solid–liquid surface tensions, θ is wetting angle, r is the pore radius of perform. A infiltration model of melt into perform was proposed and of infiltration processes were described in sketch map (Fig. 4). Owing to the pore size of preform used in the test is relatively bigger, the gravity of melt became the infiltration impetus. At initial stages, the melt occur magnitude of the

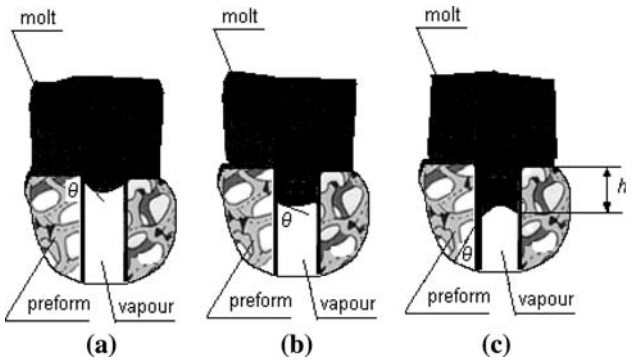

Fig. 4 Sketch map of infiltration processes

curvature under gravity driven and exhibit a forward trend (Fig. 4a), but the bad wettability became the obstacle of melt into pore channel. Owing to light chemical reactions between liquid and solid surface can result in good wetting, the wetting angle and the magnitude of the curvature turn smaller and smaller, therefore, the infiltration resistance turn smaller and smaller (Fig. 4b). Once the wetting angle $\theta < 90°$, then magnitude of the curvature begin to turn bigger in the reversed direction. Gravity overcome the infiltration resistance and molt were infiltration completely (Fig. 4c). Viewpoint of chemical reactions enhance wettability and infiltration was validated by Cirakoglu [17].

The role of oxide and Mg content

There are several methods to enhance the wettability in metal-ceramic system. Chemical wetting agents can be employed in some systems to achieve pressureless infiltration. One approach is based on coating the ceramic with another metal or treating the ceramic surface with chemical compounds. A more versatile approach is to alloy the infiltration metal. Addition of Mg into Al can improve significantly the wettability in Al–Mg–Si_3N_4 system. It can be shown in Fig. 5 that the wetting angle decreases with the increases of Mg content, for example, when Mg content is 2 wt% the wetting angle is 80°, when Mg content is 5 wt% the wetting angle is 78°, when Mg content is 8 wt% the wetting angle is 68° and when Mg content is 10 wt% the wetting angle is 60° at the temperature of 850 °C. Low content of Mg play a small role because of its low vapor pressure and prematurely lost from the system. There are two reasons to give integrated explains why the presence of Mg content can promote the infiltration. One is that magnesium element is absorbed at interface and/or surface, reduce the surface tension. Two is that light chemical reaction occurs at the interface of metal-ceramic, speed up the mass transport. Zufia [18] drew the conclusion that the content of Mg beyond 10 wt% has little further effect.

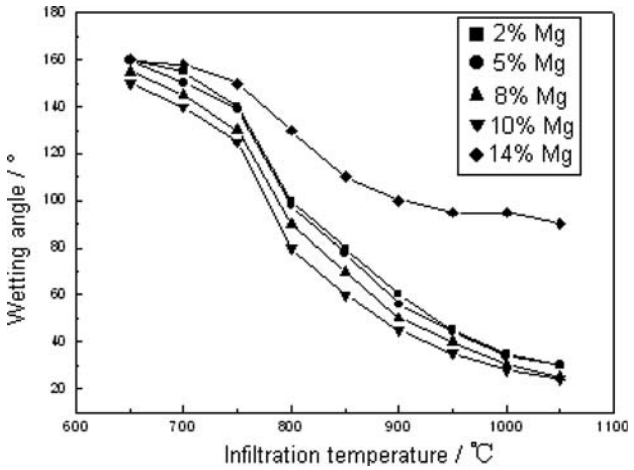

Fig. 5 The change of wetting angle with the increases of temperature at different Mg content

However, there is an adverse influence once the Mg content exceeds 10% in the Al–Mg/Si_3N_4 system. Although the wetting angle decreases with the increases of temperature, the decreases are very slow. The wetting angle is 115° at 850 °C, 98° at 850 °C and 88° at 1050 °C. In order to explain these results, it is necessary to consider the interface chemical reactions between metal and ceramic. At the interface of Al–Mg/Si_3N_4, the chemical reaction occurs as follow,

$$Mg + SiO_2 \rightarrow Si + MgO \quad \Delta G^\circ = -61.7 \text{ kJ/mol}$$

$$Mg + Si \rightarrow Mg_2Si \quad \Delta G^\circ = -16.8 \text{ kJ/mol}$$

$$2Al + SiO_2 \rightarrow Si + Al_2O_3 \quad \Delta G^\circ = -64.2 \text{ kJ/mol}$$

On the interface of metal and ceramic, Mg_2Si, MgO and Al_2O_3 at interface of metal/ceramic marked 3 in Fig. 3 were examined by XRD which were shown in Fig. 6. Above reactions take place spontaneously ($\Delta G^\circ < 0$). Overfull reaction productions as oxides on the surface of melt increase the molt viscosity and deteriorate the wettability of metal/ceramic system.

The effect of oxygen

The wettability of metal/ceramic system also depends on the concentration of oxygen. The existence of small additions of oxygen can decrease significantly the wetting angle of metal/ceramic in the literature [19]. Naidich [20] proved that the presence of oxygen lowers the contact angle of molten Cu on Al_2O_3. Travitzky [21] drew on the same conclusion, in that tests four copper–oxygen alloys with low concentrations of oxygen, i.e., 0.8, 1.6, 2.4 and 3.2 wt%, were prepared. The corresponding wetting angles were 77, 57, 44, 32°, respectively. The presence of oxygen, however, results in deterioration of wettability of Al–Mg melt with Si_3N_4. It is indicated that with the increases of oxygen concentration the wetting angle increases and weight gain decrease greatly (Fig. 7). The oxygen concentration were 0.02×10^{-3}, 0.6×10^{-3}, 1×10^{-3}, 12×10^{-3} Pa, the corresponding wetting angle were 34, 65, 83 and 91°, respectively. Synchronously, the corresponding weight gains were 60, 56, 47, 44 and 42 g, respectively. Owing to active Mg element reacts with oxygen easily and form oxides skins on the metal surface, the wettability of metal/ceramic system turn worse. Al oxides form a

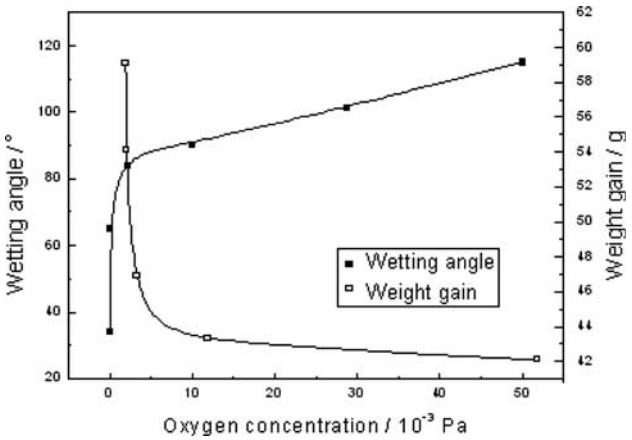

Fig. 7 The effect of oxygen on wetting angle and weight gain

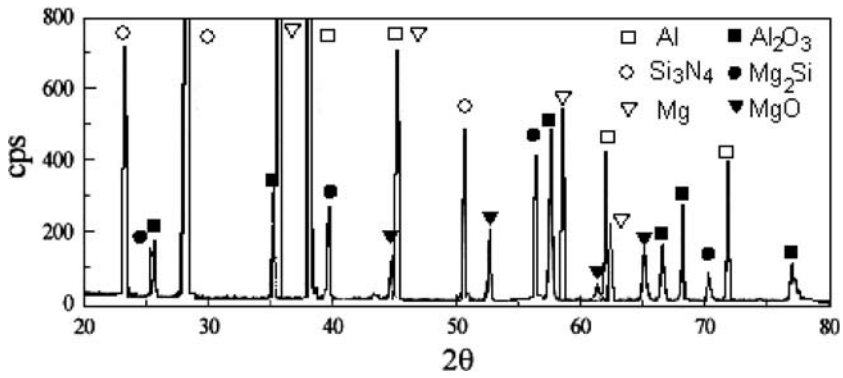

Fig. 6 XRD of 3 spot as described in Fig. 3

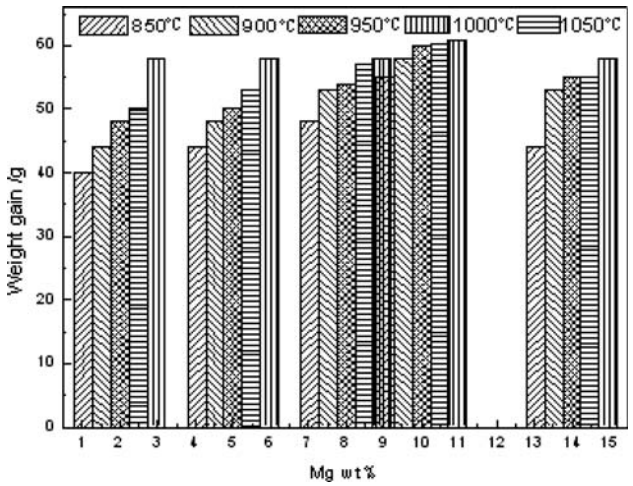

Fig. 8 The weight gain of the sample with the increases of Mg content

compact and passivating layer and Mg oxides form a porous and non-protective layer, under adequate conditions of temperature and sufficient oxygen amount, the oxides layer can advance to the liquid metal.

Infiltration temperature and infiltration time

Infiltration of Al–Mg melt with different Mg content into network structure skeleton at appointed temperature was monitored by recording the weight gain in the time of 30 min and shown in Fig. 8. From the Fig. 8, the weight gains increase with the increasing of Mg content and increase with the increasing of temperature. Similarly, the wetting angle decreases with the increasing of temperature (Fig. 5). Thermally activated force became the infiltration impetus. Figure 9 shows the cross section morphology of sample at 780, 850, 950, 1050 °C, respectively. The area of infiltration of the cross-section in samples 4 (Table 2) held at various temperatures is given in Fig. 6. There was a incomplete infiltration in Fig. 6a, b owing to the low infiltration temperature. It has been demonstrated that temperature is the factor that most significantly affects the infiltrated area, which enlarges with the increasing of temperature. When temperature reaches at 950 °C, a good infiltration area of the cross-section is observed (Fig. 9c), subsequently, when temperature reaches at 1050 °C, an excellent infiltration area of the cross-section has been obtained (Fig. 9d).

Figure 10 shows the dynamic change of weight gain at different time and different temperature and appointed Mg content as 5 wt%. It can be shown that there are three periods as incubation period, quick infiltration period and steady state period. With the increases of temperature, the incubation period became shorter. With the increases of temperature, the infiltration rate increases greatly. The infiltration rate depends intensively on the elevation of temperature in quick infiltration period. Quick infiltration period after in incubation period turn into steady state

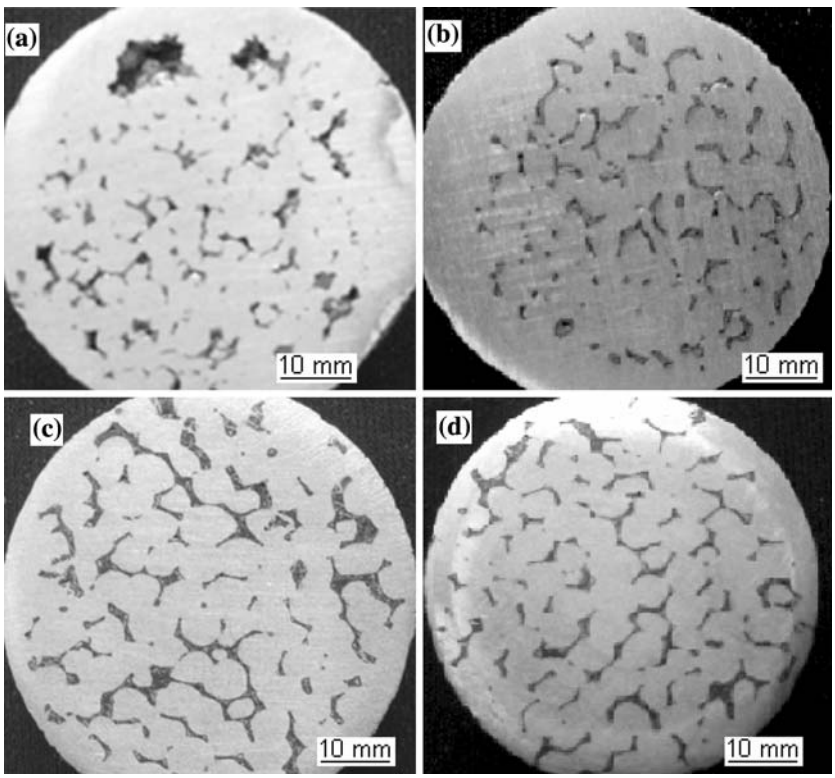

Fig. 9 The infiltration area of the cross-section in samples at various temperatures. (**a**) 780 °C (**b**) 800 °C (**c**) 950 °C (**d**) 1050 °C)

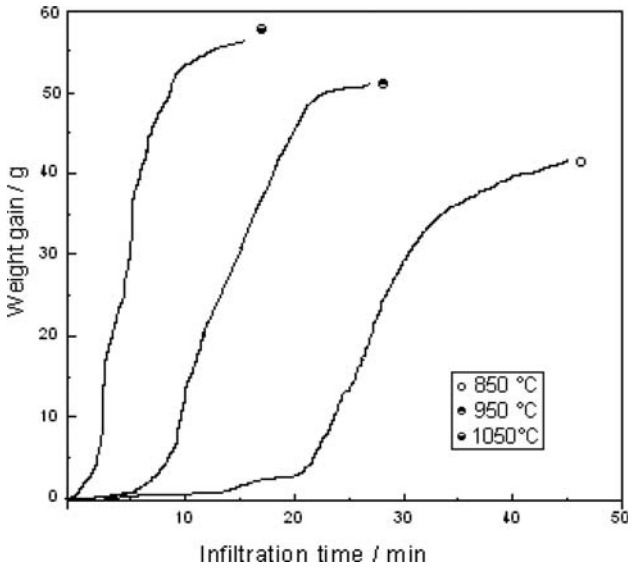

Fig. 10 Infiltration profile of Al–Mg/ Si_3N_4 system (5 wt% Mg)

period, so the infiltration profile became parabolic-type infiltration curves. The same conclusion was drown in the literature [22]. The effective infiltration time is 15 min at 1050 °C, appropriate infiltration time is 25 min at 950 °C and 45 min at 850 °C, prolonging the infiltration time continuously has no significance.

Conclusions

(1) Three dimensional network structure reinforced aluminum magnesium matrix composites had been fabricated via pressureless infiltration technology. The matrix and the reinforcement phase, form an interconnected interpenetrating network structure.

(2) Wetting angle of Al–Mg/Si_3N_4 system was taken as the critical parameters. The Al–Mg/Si_3N_4 system exhibits an excellent wettability under moderate conditions. Aluminum had a difficulty to infiltrate the perform without the volume of Mg driven in infiltration processing. The increasing of Mg content (2–10 wt%) resulted in an increased amount of infiltration however, the increasing of Mg content beyond 10 wt% has an adverse effect.

(3) The infiltration process is controlled by an interfacial mass transfer mechanism. light chemical reaction occurs in the interface of Al–Mg/Si_3N_4 system and the reaction productions reduce the surface tension of melt and impulse the infiltration. Infiltration temperature and infiltration time were the key parameters, which turn into the infiltration impetus.

Acknowledgements This work was supported by the Natural Science Foundation of Shandong Province (Y2006F03). Part of this research was done at the Institute of Materials Science Jinan University. The authors are owing a debt of gratitude to the technical staff of institutions for their help.

References

1. Wang HY, Jiang QC, Zhao YQ (2004) Mater Sci Eng A 372:109
2. Trojanova Z, Lukac P, Riehemann W, Mordike BL (2002) Mater Sci Eng A 324:122
3. Xu ZR, Chawla KK, Wolfenden A, Neuman A, Liggett GM, Chawla N (1995) Mater Sci Eng A 203:75
4. Konopka K, Olszówka-Myalska A, Szafran M (2003) Mater Chem Phys 81:329
5. Lu L, Lai MO, Froyen L (2002) Key Eng Mater 230(2):287
6. Jiang QC, Wang HY, Wang JG (2003) Mater Lett 57:2580
7. Saravanan RA, Surappa MK (2000) Mater Sci Eng A 276:108
8. Lu L, Thong KK, Gupta M (2003) Composit Sci Technol 63:627
9. Ferkel H, Mordike BL (2001) Mater Sci Eng A 298:193
10. Filho AL, Atkinson H, Jones H (1998) J Mater Sci 33:5517, Doi: 10.1023/A;1004443627023
11. Thakur SK, Dhindaw BK (2001) Wear 247:191
12. Jiang QC, Wang HY, Guan QF (2003) Adv Eng Mater 10:722
13. Wang HY, Jiang QC, Li XL (2003) Scripta Materialia 48:1349
14. Srinivasa Rao B, Jayaram V (2001) Acta Mater 49:2373
15. Trumble KP (1998) Acta Mater 46(7):2363
16. Zafer T, Thompson Derek P (2005) Mater Lett 59:1897
17. Cirakoglu M, Toy C, Tekin A, Scott WD (1997) Ceram Int 23:115
18. Zufia A, Hand RJ (2000) Mater Sci Technol 16(7):867
19. Rocher JP, Quenisset JM, Naslain R (1989) J Mater Sci 24:2697, Doi: 10.1007/BF02385613
20. Naidich YV (1981) Prog Surf Membr Sci 1:393
21. Travitzky NA, Shlayen A (1998) Mater Sci Eng A 244:154
22. Contreras A, Lopez VH, Bedolla E (2004) Scripta materialia 51:249